Journal of Applied Toxicology

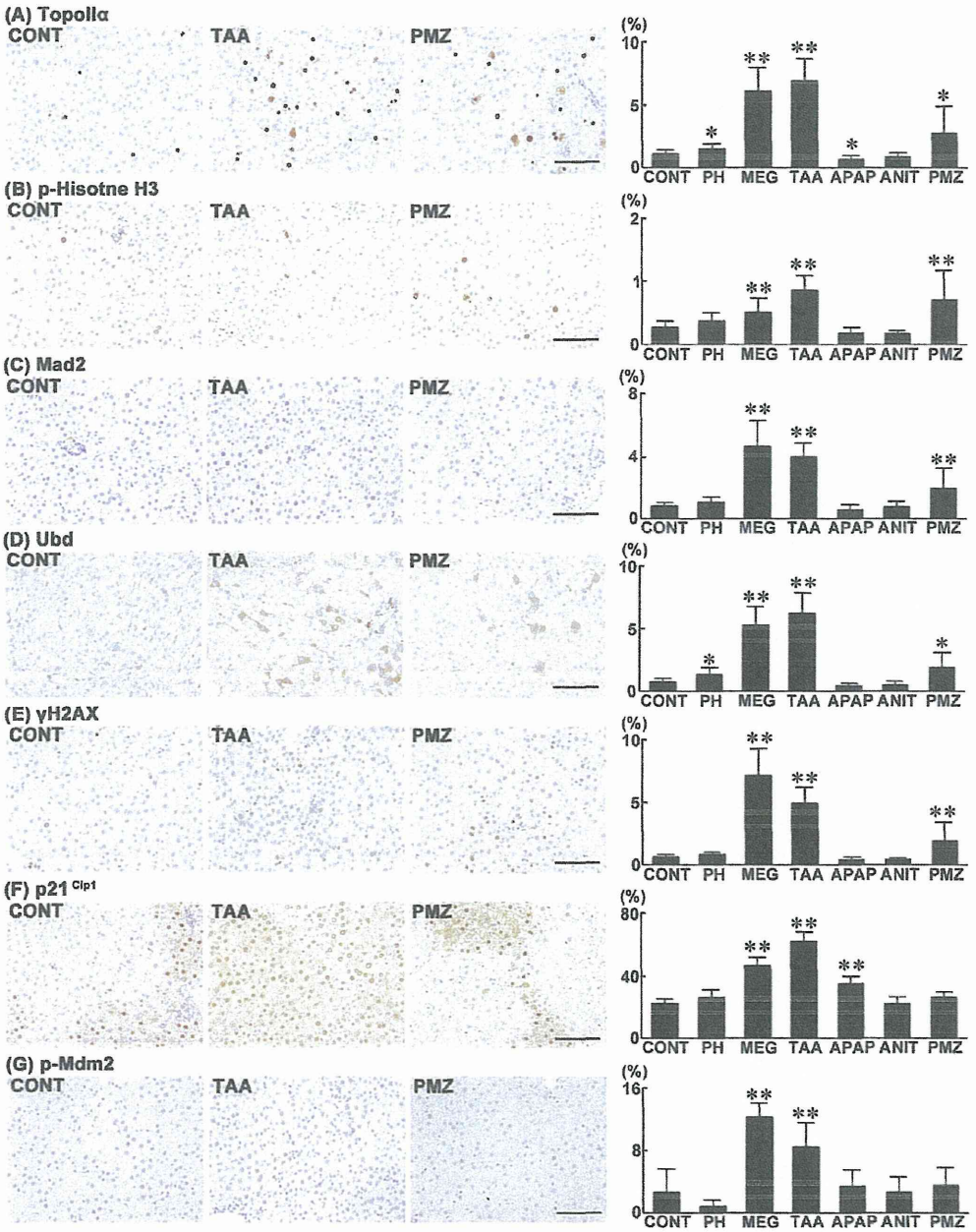

Figure 4. Distribution of Topollα^+, p-Histone H3$^+$, Mad2$^+$, Ubd$^+$, γH2AX$^+$, p21^{Cip1+} and p-Mdm2$^+$ cells in the liver of rats at day 28 after treatment with PH, noncarcinogenic hepatotoxicants or hepatocarcinogens. Photomicrographs show the distribution of Topollα^+, p-Histone H3$^+$, Mad2$^+$, Ubd$^+$, γH2AX$^+$, p21^{Cip1+} and p-Mdm2$^+$ cells in the liver of representative cases from untreated controls and animals treated with TAA or PMZ. The graphs show positive cell ratios of hepatocytes per total cells counted in 10 animals in each group. Values represent mean + SD. (A) Topoll α, (B) p-Histone H3, (C) Mad2, (D) Ubd, (E) γH2AX, (F) p21^{Cip1} and (G) p-Mdm2. Bar = 100 μm. *$P < 0.05$, **$P < 0.01$ vs. untreated controls (Dunnett's or Steel's test). ANIT, α-naphthyl isothiocyanate; APAP, acetaminophen; CONT, untreated controls; MEG, methyleugenol; PH, partial hepatectomy; PMZ, promethazine hydrochloride; TAA, thioacetamide.

compared with untreated controls. *Cdkn2a* and *Rb1* showed a significant decrease in transcript levels in the MEG, TAA and PMZ groups, compared with untreated controls. *Rbl2* showed a significant expression decrease in the MEG and TAA groups, compared with untreated controls. *Tp53* and *Mdm2* showed a significant increase in transcript levels in the TAA group, compared with untreated controls. In contrast, the transcript level of *Tp53* was significantly lower in the MEG and PMZ groups compared with untreated controls. Among the spindle checkpoint and M phase-related genes, *Aurka*, *Bub1* and *Plk1* showed a significant decrease in transcript levels in the MEG and PMZ groups, compared with untreated controls. *Aurkb* showed a significant expression decrease in the MEG, TAA and PMZ groups, compared with untreated controls. *Mad1l1* showed a significant expression decrease in the TAA group, compared with untreated controls. *Mad2l1* showed a significant expression decrease in the PMZ group, compared with untreated controls. Among the DNA damage-related genes, *Atm* and *Chek1* showed a significant decrease in transcript levels in the PMZ group, compared with untreated controls. *Brca1* showed a significant expression decrease in the MEG, TAA and PMZ groups, compared with untreated controls. *Brca2*, *Chek2* and *Esco1* showed a significant decrease in transcript levels in the MEG and PMZ groups, compared with untreated controls. *Brcc3* showed a significant expression decrease in the TAA and PMZ groups, compared

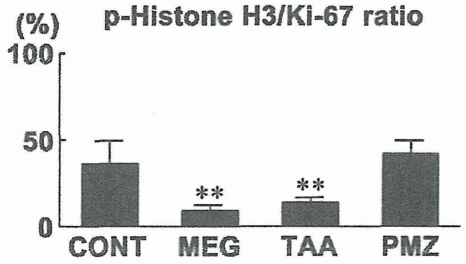

Figure 5. p-Histone $H3^+$/Ki-67^+ cell ratio in the liver of rats at day 28 after treatment with MEG, TAA or PMZ. The graph shows p-Histone $H3^+$ cell ratio of hepatocytes per Ki-67^+ cells counted in 10 animals in each group. Values represent mean + SD. $^{**}P < 0.01$ vs. untreated controls (Steel's test). CONT, untreated controls; MEG, methyleugenol; PMZ, promethazine hydrochloride; TAA, thioacetamide.

with untreated controls. *Esco1* and *Rad17* showed a significant increase in transcript levels in the TAA group, compared with untreated controls. *Gadd45a* showed a significant expression increase in the TAA and PMZ groups, compared with untreated controls. *Rad50* did not change the transcript level in any of the treatment groups.

At day 7, *Cdkn1a* and *Mdm2* showed a significant increase in transcript levels in the MEG and TAA groups compared with untreated controls, among the G_1/S checkpoint-related genes. In contrast, the transcript level of *Cdkn1a* was significantly lower in the PMZ group compared with untreated controls. *Cdkn2a* and *Tp53* showed a significant decrease in transcript levels in the MEG and PMZ groups, compared with untreated controls. In contrast, the transcript level of *Tp53* was significantly higher in the TAA group compared with untreated controls. *Rb1* and *Rbl2* showed a

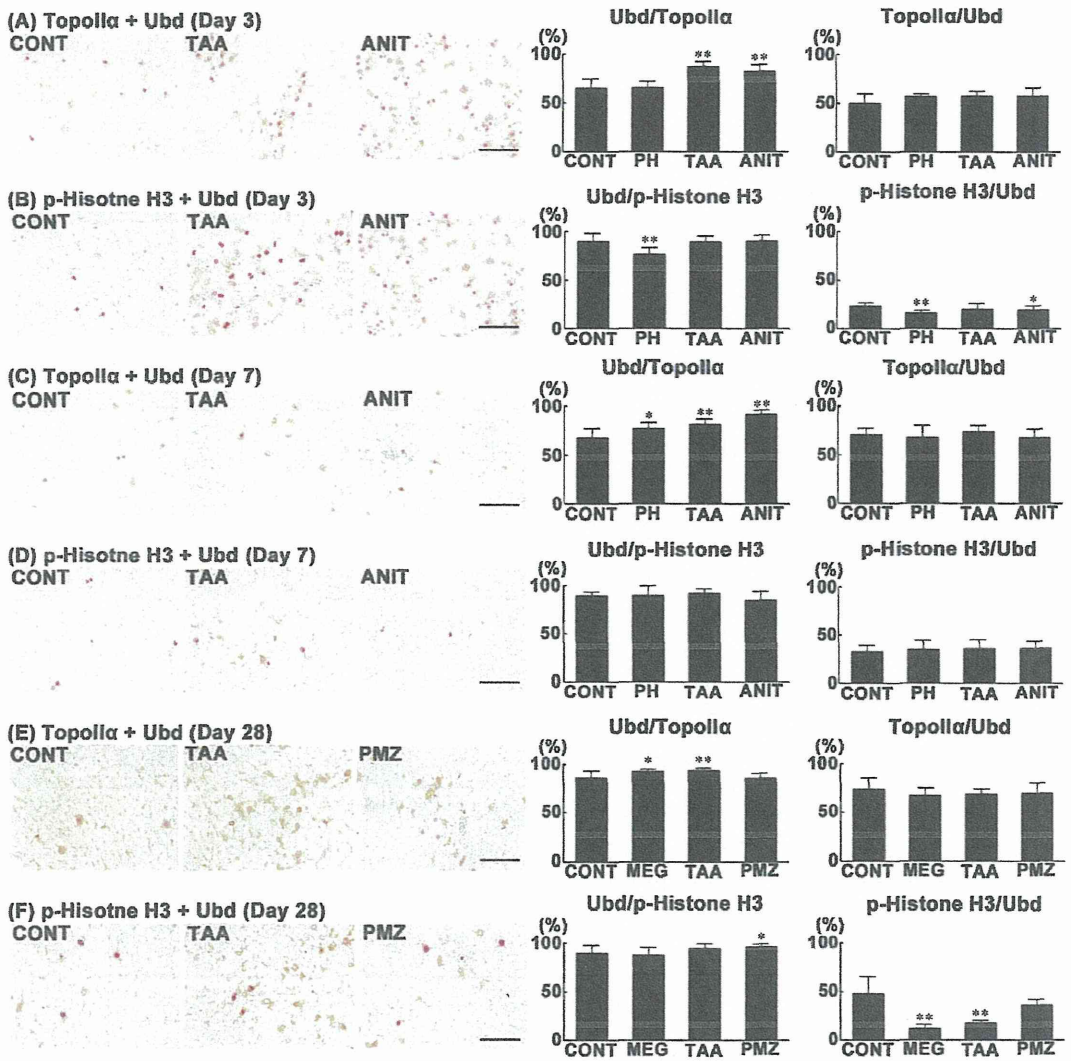

Figure 6. Distribution of immunoreactive cell populations of TopoⅡα co-expressing Ubd (Ubd/TopoⅡα), Ubd co-expressing TopoⅡα (TopoⅡα/Ubd), p-Histone H3 co-expressing Ubd (Ubd/p-Histone H3) or Ubd co-expressing p-Histone H3 (p-Histone H3/Ubd) in the liver of rats at days 3, 7 and 28. Photomicrographs show the distribution of Ubd/TopoⅡα, TopoⅡα/Ubd, Ubd/p-Histone H3 and p-Histone H3/Ubd in the liver of untreated controls (A–F), animals treated with TAA or ANIT (A–D), and animals treated with TAA or PMZ (E,F). The immunoreactivity of Ubd (cytoplasm), and p-Histone H3 (nucleus) or TopoⅡα (nucleus) is visualized as brown and red, respectively. The graphs show the Ubd-positive cell ratio (%) per total liver cells immunoreactive with TopoⅡα or p-Histone H3, and the TopoⅡα or p-Histone H3-positive cell ratio (%) per total liver cells immunoreactive with Ubd counted in 10 animals in each group. Values represent mean + SD. (A) Ubd/TopoⅡα and TopoⅡα/Ubd, (B) Ubd/p-Histone H3 and p-Histone H3/Ubd (day 3), (C) Ubd/TopoⅡα and TopoⅡα/Ubd (day 7), (D) Ubd/p-Histone H3 and p-Histone H3/Ubd (day 7), (E) Ubd/TopoⅡα and TopoⅡα/Ubd (day 28), (F) Ubd/p-Histone H3 and p-Histone H3/Ubd (day 28). Bar = 100 μm. $^{*}P < 0.05$, $^{**}P < 0.01$, vs. untreated controls (Dunnett's or Steel's test). ANIT, α-naphthyl isothiocyanate; CONT, untreated controls; MEG, methyleugenol; PMZ, promethazine hydrochloride; TAA, thioacetamide.

Table 4. Relative transcript levels in the liver of rats treated with MEG, TAA or PMZ for up to 28 days

Gene	Day 3			Day 7			Day 28		
	MEG[a]	TAA[a]	PMZ[a]	MEG[a]	TAA[a]	PMZ[a]	MEG[a]	TAA[a]	PMZ[a]
G_1/S checkpoint-related genes									
Cdkn1a	2.13 ± 0.59[b,**]	2.61 ± 0.38**	0.41 ± 0.13**	2.14 ± 0.43**	2.21 ± 0.26**	0.30 ± 0.07**	2.67 ± 0.40**	2.99 ± 0.62**	0.28 ± 0.08**
Cdkn2a	0.32 ± 0.18*	0.47 ± 0.31*	0.43 ± 0.29*	0.57 ± 0.46*	0.70 ± 0.28	0.47 ± 0.37*	1.58 ± 0.49	2.52 ± 0.19**	0.73 ± 0.15
Rb1	0.54 ± 0.33*	0.52 ± 0.10**	0.30 ± 0.09**	0.49 ± 0.09**	0.52 ± 0.07**	0.55 ± 0.04**	0.79 ± 0.05	0.40 ± 0.06**	0.57 ± 0.15**
Rbl2	0.55 ± 0.28*	0.33 ± 0.06**	0.65 ± 0.32	0.42 ± 0.07**	0.30 ± 0.04**	0.70 ± 0.15*	0.55 ± 0.06**	0.33 ± 0.04**	0.82 ± 0.14
Mdm2	2.86 ± 1.65	3.36 ± 0.64**	0.86 ± 0.35	4.55 ± 0.76**	3.75 ± 0.67**	0.85 ± 0.14	3.74 ± 1.13**	3.20 ± 0.36**	0.90 ± 0.14
Tp53	0.73 ± 0.34*	1.51 ± 0.19**	0.49 ± 0.10**	0.64 ± 0.11**	1.41 ± 0.18**	0.67 ± 0.12**	0.96 ± 0.08	1.63 ± 0.27**	0.99 ± 0.11
Spindle checkpoint and M phase-related genes									
Aurka	0.22 ± 0.12**	1.27 ± 0.38	0.13 ± 0.04**	0.36 ± 0.07**	0.87 ± 0.18	0.80 ± 0.36	1.34 ± 0.32	1.96 ± 0.26**	1.03 ± 0.31
Aurkb	0.34 ± 0.31*	0.42 ± 0.34*	0.02 ± 0.01**	0.21 ± 0.07**	0.30 ± 0.07**	0.58 ± 0.45	2.61 ± 0.82**	1.87 ± 0.36*	1.12 ± 0.36
Bub1	0.17 ± 0.10**	0.79 ± 0.31	0.08 ± 0.02**	0.23 ± 0.08**	0.38 ± 0.09**	0.75 ± 0.42	2.16 ± 0.52**	1.50 ± 0.15	1.22 ± 0.36
Mad1l1	0.73 ± 0.32	0.56 ± 0.10**	0.72 ± 0.27	0.60 ± 0.06**	0.49 ± 0.07**	0.80 ± 0.14**	0.93 ± 0.29	0.52 ± 0.07**	0.87 ± 0.11
Mad2l1	0.75 ± 0.57	0.69 ± 0.47	0.16 ± 0.05**	0.43 ± 0.07**	0.95 ± 0.17	0.66 ± 0.32	2.18 ± 0.64**	2.68 ± 0.43**	1.25 ± 0.34
Plk1	0.13 ± 0.09**	0.94 ± 0.34	0.02 ± 0.01**	0.21 ± 0.09**	0.36 ± 0.11**	0.85 ± 0.56	2.24 ± 0.83**	1.92 ± 0.37**	1.21 ± 0.35
DNA damage-related genes									
Atm	0.79 ± 0.32	0.92 ± 0.18	0.67 ± 0.22*	0.71 ± 0.07	0.78 ± 0.09	0.94 ± 0.11	0.76 ± 0.10*	0.95 ± 0.08	0.88 ± 0.11
Brca1	0.27 ± 0.15**	0.76 ± 0.25*	0.25 ± 0.12**	0.24 ± 0.03**	0.47 ± 0.08**	0.68 ± 0.26	1.18 ± 0.31	0.97 ± 0.07	0.87 ± 0.14
Brca2	0.48 ± 0.26*	1.19 ± 0.39	0.26 ± 0.09**	0.54 ± 0.12**	1.03 ± 0.25	0.91 ± 0.37	0.73 ± 0.06	0.72 ± 0.06	0.86 ± 0.13
Brcc3	0.78 ± 0.41	0.76 ± 0.10**	0.70 ± 0.25*	0.62 ± 0.09**	0.67 ± 0.09**	0.57 ± 0.12**	1.87 ± 0.37*	3.17 ± 0.86**	1.37 ± 0.40
Chek1	0.73 ± 0.42	0.81 ± 0.41	0.30 ± 0.11**	0.61 ± 0.08**	1.06 ± 0.22	0.93 ± 0.15	1.98 ± 0.48**	1.94 ± 0.27**	1.24 ± 0.28
Chek2	0.45 ± 0.22**	1.28 ± 0.36	0.36 ± 0.16**	0.46 ± 0.03**	1.27 ± 0.26	0.84 ± 0.17	0.84 ± 0.29	1.29 ± 0.11	0.70 ± 0.13
Esco1	0.70 ± 0.35*	1.53 ± 0.25**	0.57 ± 0.15**	0.51 ± 0.05**	1.74 ± 0.21**	0.72 ± 0.18**	0.61 ± 0.12**	1.51 ± 0.15**	0.59 ± 0.09**
Gadd45a	1.88 ± 1.31	3.18 ± 0.61**	1.97 ± 0.11**	1.10 ± 0.25	2.35 ± 0.46**	0.47 ± 0.14**	1.83 ± 0.56	3.07 ± 0.50**	1.18 ± 0.63
Rad17	0.89 ± 0.45	1.94 ± 0.29**	0.79 ± 0.17	0.69 ± 0.12**	2.20 ± 0.23**	0.65 ± 0.17**	0.88 ± 0.07	2.15 ± 0.17**	0.74 ± 0.09**
Rad50	0.94 ± 0.50	1.18 ± 0.26	0.62 ± 0.22	0.71 ± 0.15**	1.00 ± 0.13	0.80 ± 0.22	0.85 ± 0.08	1.27 ± 0.14**	0.95 ± 0.10

Atm, ATM serine/threonine kinase; Aurka, aurora kinase A; Aurkb, aurora kinase B; Brca1, breast cancer 1, early onset; Brca2, breast cancer 2, early onset; Brcc3, BRCA1/BRCA2-containing complex, subunit 3; Bub1, BUB1 mitotic checkpoint serine/threonine kinase; Cdkn1a, cyclin-dependent kinase inhibitor 1A; Cdkn2a, cyclin-dependent kinase inhibitor 2A; Chek1, checkpoint kinase 1; Chek2, checkpoint kinase 2; Esco1, establishment of sister chromatid cohesion N-acetyltransferase 1; Gadd45a, growth arrest and DNA-damage-inducible, alpha; Mad1l1, MAD1 mitotic arrest deficient-like 1 (yeast); Mad2l1, MAD2 mitotic arrest deficient-like 1 (yeast); Mdm2, MDM2 proto-oncogene, E3 ubiquitin protein ligase; MEG, methyleugenol; Plk1, polo-like kinase 1; PMZ, promethazine hydrochloride; Rad17, RAD17 homolog (S. pombe); Rad50, RAD50 homolog (S. cerevisiae); Rb1, retinoblastoma 1; Rbl2, retinoblastoma-like 2; TAA, thioacetamide; Tp53, tumor protein p53.

[a] $n = 6$.

[b] Values represent relative expression levels expressed as mean ± SD.

* $P < 0.05$, ** $P < 0.01$ vs. untreated controls (Dunnett's or Steel's test).

significant decrease in transcript levels in the MEG, TAA and PMZ groups, compared with untreated controls. Among the spindle checkpoint and M phase-related genes, *Aurka* and *Mad2l1* showed a significant decrease in transcript levels in the MEG group, compared with untreated controls. *Aurkb*, *Bub1* and *Plk1* showed a significant decrease in transcript levels in the MEG and TAA groups, compared with untreated controls. *Mad1l1* showed a significant expression decrease in the MEG, TAA and PMZ groups, compared with untreated controls. Among the DNA damage-related genes, *Brca1* showed a significant expression decrease in the MEG and TAA groups, compared with untreated controls. *Brca2*, *Chek1* and *Chek2* showed a significant decrease in transcript levels in the MEG group, compared with untreated controls. *Brcc3* showed a significant expression decrease in the MEG, TAA and PMZ groups, compared with untreated controls. *Esco1* and *Rad17* showed a significant decrease in transcript levels in MEG and PMZ groups, compared with untreated controls. In contrast, the transcript levels of *Esco1*, *Gadd45a* and *Rad17* were significantly higher in the TAA group compared with untreated controls. *Gadd45a* showed a significant expression decrease in the PMZ group, compared with untreated controls. *Rad50* showed a significant expression decrease in the MEG group, compared with untreated controls. *Atm* did not change the transcript level in any of the treatment groups.

At day 28, *Cdkn1a* and *Mdm2* showed a significant increase in transcript levels in the MEG and TAA groups compared with untreated controls, among the G_1/S checkpoint-related genes. In contrast, the transcript level of *Cdkn1a* was significantly lower in the PMZ group compared with untreated controls. *Cdkn2a* and *Tp53* showed a significant increase of expression in the TAA group, compared with untreated controls. *Rbl2* showed a significant expression decrease in the MEG and TAA groups, compared with untreated controls. *Rb1* showed a significant expression decrease in the TAA and PMZ groups, compared with untreated controls. Among the spindle checkpoint and M phase-related genes, *Aurkb*, *Mad2l1* and *Plk1*showed a significant increase of expression in the MEG and TAA groups, compared with untreated controls. *Aurka* showed a significant increase of expression and *Mad1l1* showed a significant expression decrease in the TAA group, compared with untreated controls. *Bub1* showed a significant increase of expression in the MEG group, compared with untreated controls. Among the DNA damage-related genes, *Brcc3* and *Chek1* showed a significant increase of expression in the MEG and TAA groups, compared with untreated controls. *Esco1*, *Gadd45a*, *Rad17* and *Rad50* showed a significant increase in transcript levels in the TAA group, compared with untreated controls. *Atm* and *Esco1* showed a significant decrease in transcript levels in the MEG group, compared with untreated controls. *Esco1* and *Rad17* showed significant decrease in transcript levels in PMZ group as compared with untreated controls. *Brca1*, *Brca2* and *Chek2* did not change the transcript level in any of the treatment groups.

Discussion

In the present study, we observed an unchanged or a decreased number of Ki-67$^+$ liver cells and increased numbers of nuclear p21^{Cip1+} cells and cleaved caspase 3$^+$ cells at day 7 of treatment with most chemicals irrespective of their carcinogenic potential. In contrast, only hepatocarcinogens increased the numbers of nuclear p21^{Cip1+} cells concomitantly with facilitation of apoptosis and cell proliferation after 28 days of treatment. Considering p21^{Cip1} is one of the cyclin-dependent kinase inhibitors that leads to cell cycle arrest at G_1 phase in response to a variety of stimuli, such as DNA damage, oxidative stress and cytokine action (Abbas & Dutta, 2009; Gorospe *et al.*, 1999; Rodriguez & Meuth, 2006; Sherr & Roberts, 1995), the increase in nuclear p21^{Cip1+} cells in the present study suggests promotion of G_1/S arrested cells. We also found that hepatocarcinogens increased the mRNA expression of *Brcc3*, encoding a molecule repairing DNA damage by activating *Brca1* (Chen *et al.*, 2006), and *Chek1*, encoding a DNA damage checkpoint molecule (Patil *et al.*, 2013), after 28 days of treatment. In contrast, hepatocarcinogens did not increase the mRNA expression of *Brcc3* and *Chek1* at day 3 and reflecting accumulation of DNA damage at day 28 of hepatocarcinogen treatment, whereas activation of this molecule at earlier time points of hepatocarcinogen treatment may not be related to DNA damage. Activation of p21^{Cip1} may also be responsible for facilitation of apoptosis as revealed by the increase in the number of cleaved caspase 3$^+$ cells from day 7 of treatment with hepatocarcinogens, because p21^{Cip1} is a prerequisite for the induction of apoptosis (Kondo *et al.*, 1996; Lincet *et al.*, 2000). Activation of p21^{Cip1} at earlier time points may be the reflection of cellular toxicity by carcinogenic chemicals, because noncarcinogenic APAP and ANIT also increased p21^{Cip1+} cells and apoptosis at day 7. While the noncarcinogenic PMZ also caused an increase in the number of Ki-67$^+$ proliferating cells, this hepatotoxicant did not increase apoptosis, the number of p21^{Cip1+} cells and mRNA expression of genes encoding DNA repair enzymes or DNA damage checkpoint molecule at day 28. Therefore, the increase in apoptosis and p21^{Cip1+} cells may be the signature of cellular responses against treatment with hepatocarcinogens evoking cell proliferation, as reported previously (Yafune *et al.*, 2013a). Twenty-eight days may be sufficient for distinguishing between hepatocarcinogens and nonhepatocarcinogens facilitating cell proliferation at the end of this period.

In the present study, the hepatocarcinogens downregulated the expression of *Rbl2* at all time points, a gene encoding one of the Rb family proteins that regulate the progression of G_1/S phase (Cobrinik, 2005; Cobrinik *et al.*, 1996). However, noncarcinogenic PMZ also downregulated *Rbl2* on day 7, suggesting that the downregulation of *Rbl2* expression at earlier time points may not be carcinogen specific. Interestingly, PMZ increased cell proliferation accompanied with an apparent increase in cells expressing Topollα, p-Histone H3, Mad2, Ubd and γH2AX at day 28; however, the transcript level of *Rbl2* was unchanged with untreated controls at this time point. These results suggest the hepatocarcinogen-specific disruption of G_1/S checkpoint function in subpopulations of liver cells, leading to S phase progression, which may appear at day 28 of treatment. Downregulation of *Rbl2* has been observed in human breast and endometrial cancers (Milde-Langosch *et al.*, 2001). In the present study, hepatocarcinogens upregulated or tended to upregulate *Mdm2*, a p53 downstream molecule that facilitates degradation of both p53 and Rb protein through facilitation of ubiquitination (Bhattacharya & Ghosh, 2014; Honda *et al.*, 1997; Uchida *et al.*, 2005) at all time points of measurements. In addition, hepatocarcinogens also increased cells immunoreactive with Mdm2 phosphorylated at Ser 166, an activated isoform of Mdm2 that can translocate from the cytoplasm to the nucleus for facilitation of p53 degradation (Malmlöf *et al.*, 2007; Mayo & Donner, 2002), in parallel with transcript upregulation. We have previously shown that hepatocarcinogens promoting liver cell proliferation increased the number of p53$^+$ liver cells, which is indicative of the induction of *Mdm2* transcription (Yafune *et al.*, 2013a). On the other hand, noncarcinogenic APAP and PMZ also increased p-Mdm2$^+$ cell populations at day 7, but not at day 28. Therefore, hepatocarcinogen-specific *Mdm2* transcript upregulation and increase of nuclear p-Mdm2 expression, suggesting the facilitation of

Journal of Applied Toxicology

proteosomal degradation of p53 and Rb proteins, may appear by 28 days of treatment. p53 is known to be upregulated and activated by genotoxic stress to induce cell cycle arrest at G_1 phase by induction of a number of genes including the $p21^{Cip1}$ to repair DNA damage (Bartek & Lukas, 2001; Speidel, 2015). Increase of $p21^{Cip1+}$ cells and upregulation of *Cdkn1a*, *Brcc3* and *Chek1* genes by hepatocarcinogen treatment in the present study may reflect accumulation of DNA damage probably in association with p53 degradation.

As previously discussed (Taniai *et al.*, 2012b), overexpression of Ubd results in suppression of the kinetochore localization of Mad2 at the spindle checkpoint during M phase, which may eventually lead to chromosomal instability (Herrmann *et al.*, 2007; Lim *et al.*, 2006). We previously reported aberrant expression of Ubd from G_2 phase by 28 days treatment with carcinogens that facilitate cell proliferation, suggestive of disruption of spindle checkpoint function (Taniai *et al.*, 2012b). In the present study, we revealed that MEG and TAA slightly increased the number of Ubd^+ cells within the Topollα^+ cell population at day 28, while these hepatocarcinogens did not change the number of Ubd^+ cells within the p-Histone $H3^+$ cell population at this time point, using double immunohistochemistry. Because of the Topollα expression at G_2 and M phases, and the p-Histone H3 expression at M phase (Adachi *et al.*, 1997; Beekman *et al.*, 2006; Lee *et al.*, 2004; Woessner *et al.*, 1991), our results suggest a slight increase in Ubd^+ cells at G_2 phase by hepatocarcinogens as previously reported (Taniai *et al.*, 2012b). On the other hand, MEG and TAA profoundly decreased the number of p-Histone $H3^+$ cells within the Ubd^+ cell population, while these hepatocarcinogens did not change the number of Topollα^+ cells within the Ubd^+ cell population. It is also reported that the Ubd-Mad2 interaction reduces the proportion of cells at M phase within the proliferating cell population and induces abnormalities in chromosome structure and number reflecting the disruption of the spindle checkpoint (Theng *et al.*, 2014). Our current results suggest that hepatocarcinogens cause aberrant expression of Ubd from as early as the G_2 phase, which may lead to its excess functioning before the normal timing at the spindle checkpoint. These changes were carcinogen-specific, as they were not observed with PMZ. In addition, we observed that hepatocarcinogens decreased the p-Histone $H3^+$/$Ki\text{-}67^+$ cell ratio at day 28, suggesting that hepatocarcinogens that promote liver cell proliferation lead to incomplete spindle checkpoint function, which allows acceleration of M phase transition with the onset time point as early as 28 days after starting treatment in rats. Because PH and ANIT did not profoundly decrease the number of cells in the Ubd^+ population staying at M phase at day 3, irrespective of their high cell proliferation activity, withdrawal of proliferating cells from M phase was considered specific to carcinogen-induced cell proliferation after 28 days of treatment.

With regard to expression of genes coding spindle checkpoint molecules or M phase molecules, MEG, TAA and PMZ reduced or did not change the expression of *Aurka*, *Aurkb*, *Bub1*, *Mad1l1*, *Mad2l1* and *Plk1* at days 3 and 7. At day 28, MEG increased the expression of *Aurkb*, *Bub1*, *Mad2l1* and *Plk1*, and TAA increased the expression of *Aurka*, *Aurkb*, *Mad2l1* and *Plk1*. On the other hand, PMZ did not increase the expression of these genes. The spindle checkpoint is activated by sister chromatid mis-segregation and stops the cell cycle until each and every kinetochore becomes attached to the mitotic spindle, which prevents aneuploidy (Weaver & Cleveland, 2005). Overexpression of these M phase-related genes has been observed in cultured cell lines established from breast cancer or laryngeal cancer, as well as neoplastic cells in laryngeal cancers, gastric cancers and bladder cancers, in association with increased chromosomal instability and tumor malignancy (Honma *et al.*, 2014; Yamamoto *et al.*, 2006; Yuan *et al.*, 2006; Zhang *et al.*, 2012). These results suggest that overexpression of M phase-related genes induced by 28-day treatment with carcinogens may reflect the presence of an M phase-arrested hepatocyte population by activation of the spindle checkpoint, to protect against chromosomal aberration, in addition to the proliferating hepatocyte population disrupting the spindle checkpoint.

It has been reported that partial hepatectomy induces cell proliferation at 2–4 days after treatment, and then cell proliferation activity decreases from 6 days after treatment (Gerlach *et al.*, 1997; Kunimoto *et al.*, 2009). In the present study, we compared the time course of cellular responses associated with cell proliferation of carcinogenic target cells induced by hepatocarcinogens and regenerative cell proliferation induced by PH or treatment with noncarcinogenic hepatotoxicants. We found that PH and the noncarcinogenic APAP and ANIT increased liver cell proliferation activity only at day 3, and PMZ increased it only at day 28. None of these treatments promoted cell proliferation accompanied by $p21^{Cip1}$ activation at day 28, in contrast to the concomitant facilitation of cell proliferation and $p21^{Cip1}$ activation by the hepatocarcinogenic MEG and TAA. These results suggest that $p21^{Cip1}$ activation is the signature of G_1/S checkpoint disruption caused by transcript downregulation of *Rbl2* and sequestration of Rb protein, which allows continuous facilitation of cell proliferation by hepatocarcinogens. In contrast, some feedback mechanism may be operated in the suppression of cell proliferation in the cases of PH and noncarcinogenic hepatotoxicants at day 28 without $p21^{Cip1}$ activation. For example, it has been reported that liver cell regeneration after PH is suppressed by SOCS3, which negatively regulates the cytokine signaling cascade (Riehle *et al.*, 2008).

In conclusion, it may take 28 days to induce hepatocarcinogen-specific cellular responses. Disruption of the G_1/S checkpoint

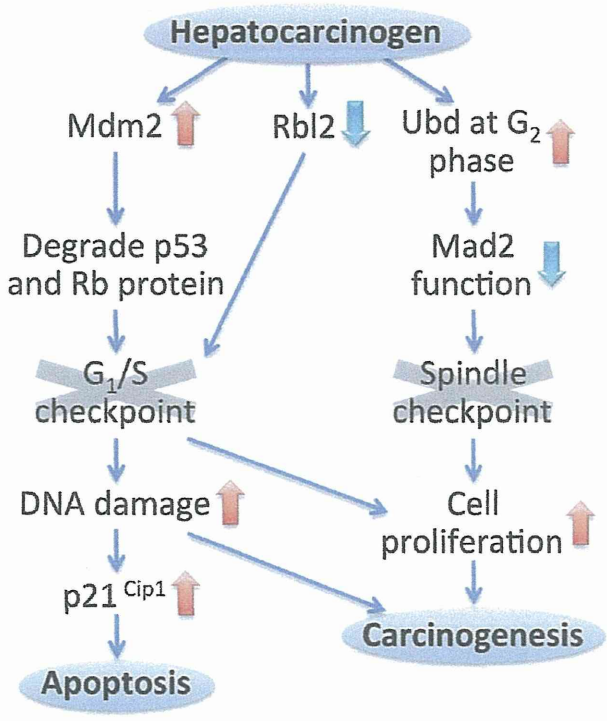

Figure 7. Hypothetical model of aberrations in cell cycle regulation specific to hepatocarcinogens to facilitate cell proliferation at day 28 of repeated administration.

function reflected by downregulation of *Rbl2*, upregulation of *Mdm2* and increase of p-Mdm2^{+} cells suggestive of sequestration of p53 and Rb protein may be responsible for facilitation of carcinogen-induced cell proliferation at day 28. Reduction in proliferating cells staying at M phase suggests early withdrawal of proliferating cells from M phase, because of disruptive spindle checkpoint function as evidenced by reduction of Ubd^{+} cells staying at M phase. Accumulation of DNA damage probably in association with facilitation of p53 degradation by activation of Mdm2 may be a prerequisite for aberrant p21^{Cip1} activation, which is responsible for apoptosis (Fig. 7).

Acknowledgments

The authors thank Mrs. Shigeko Suzuki for her technical assistance in preparing the histological specimens. This work was supported by Health and Labour Sciences Research Grants (Research on Food Safety) from the Ministry of Health, Labour and Welfare of Japan (Grant No. H25-shokuhin-ippan-005). Masayuki Kimura is a Research Fellow of the Japan Society for the Promotion of Science.

Conflict of Interest

The authors did not report any conflict of interest.

References

Abbas T, Dutta A. 2009. p21 in cancer: intricate networks and multiple activities. *Nat. Rev. Cancer* **9**: 400–414.

Adachi N, Kobayashi M, Koyama H. 1997. Cell cycle-dependent regulation of the mouse DNA topoisomerase IIα gene promoter. *Biochem. Biophys. Res. Commun.* **230**: 105–109.

Adler M, Müller K, Rached E, Dekant W, Mally A. 2009. Modulation of key regulators of mitosis linked to chromosomal instability is an early event in ochratoxin A carcinogenicity. *Carcinogenesis* **30**: 711–719.

Allen DG, Pearse G, Haseman JK, Maronpot RR. 2004. Prediction of rodent carcinogenesis: an evaluation of prechronic liver lesions as forecasters of liver tumors in NTP carcinogenicity studies. *Toxicol. Pathol.* **32**: 393–401.

Bartek J, Lukas J. 2001. Mammalian G1- and S-phase checkpoints in response to DNA damage. *Curr. Opin. Cell Biol.* **13**: 738–747.

Becker FF. 1983. Thioacetamide hepatocarcinogenesis. *J. Natl. Cancer Inst.* **71**: 553–558.

Beekman C, Nichane M, De Clercq S, Maetens M, Floss T, Wurst W, Bellefroid E, Marine JC. 2006. Evolutionarily conserved role of nucleostemin: controlling proliferation of stem/progenitor cells during early vertebrate development. *Mol. Cell. Biol.* **26**: 9291–9301.

Bhattacharya S, Ghosh MK. 2014. HAUSP, a novel deubiquitinase for Rb - MDM2 the critical regulator. *FEBS J.* **281**: 3061–3078.

Burma S, Chen BP, Murphy M, Kurimasa A, Chen DJ. 2001. ATM phosphorylates histone H2AX in response to DNA double-strand breaks. *J. Biol. Chem.* **276**: 42462–42467.

Chen X, Arciero CA, Wang C, Broccoli D, Godwin AK. 2006. BRCC36 is essential for ionizing radiation-induced BRCA1 phosphorylation and nuclear foci formation. *Cancer Res.* **66**: 5039–5046.

Clawson GA, Blankenship LJ, Rhame JG, Wilkinson DS. 1992. Nuclear enlargement induced by hepatocarcinogens alters ploidy. *Cancer Res.* **52**: 1304–1308.

Cobrinik D. 2005. Pocket proteins and cell cycle control. *Oncogene* **24**: 2796–2809.

Cobrinik D, Lee MH, Hannon G, Mulligan G, Bronson RT, Dyson N, Harlow E, Beach D, Weinberg RA, Jacks T. 1996. Shared role of the pRB-related p130 and p107 proteins in limb development. *Genes Dev.* **10**: 1633–1644.

Eastin WC. 1998. The U.S. National toxicology program evaluation of transgenic mice as predictive models for identifying carcinogens. *Environ. Health Perspect.* **106**: 81–84.

Eckle VS, Buchmann A, Bursch W, Schulte-Hermann R, Schwarz M. 2004. Immunohistochemical detection of activated caspases in apoptotic hepatocytes in rat liver. *Toxicol. Pathol.* **32**: 9–15.

Gerlach C, Sakkab DY, Scholzen T, Dassler R, Alison MR, Gerdes J. 1997. Ki-67 expression during rat liver regeneration after partial hepatectomy. *Hepatology* **26**: 573–578.

Gorospe M, Wang X, Holbrook NJ. 1999. Functional role of p21 during the cellular response to stress. *Gene Expr.* **7**: 377–385.

Herrmann J, Lerman LO, Lerman A. 2007. Ubiquitin and ubiquitin-like proteins in protein regulation. *Circ. Res.* **100**: 1276–1291.

Hirota T, Lipp JJ, Toh BH, Peters JM. 2005. Histone H3 serine 10 phosphorylation by Aurora B causes HP1 dissociation from heterochromatin. *Nature* **438**: 1176–1180.

Honda R, Tanaka H, Yasuda H. 1997. Oncoprotein MDM2 is a ubiquitin ligase E3 for tumor suppressor p53. *FEBS Lett.* **420**: 25–27.

Honma K, Nakanishi R, Nakanoko T, Ando K, Saeki H, Oki E, Iimori M, Kitao H, Kakeji Y, Maehara Y. 2014. Contribution of Aurora-A and -B expression to DNA aneuploidy in gastric cancers. *Surg. Today* **44**: 454–461.

Ichijima Y, Yoshioka K, Yoshioka Y, Shinohe K, Fujimori H, Unno J, Takagi M, Goto H, Inagaki M, Mizutani S, Teraoka H. 2010. DNA lesions induced by replication stress trigger mitotic aberration and tetraploidy development. *PLoS One* **5**: e8821.

Kondo S, Barna BP, Kondo Y, Tanaka Y, Casey G, Liu J, Morimura T, Kaakaji R, Peterson JW, Werbel B, Barnett GH. 1996. WAF1/CIP1 increases the susceptibility of p53 non-functional malignant glioma cells to cisplatin-induced apoptosis. *Oncogene* **13**: 1279–1285.

Kops GJ, Foltz DR, Cleveland DW. 2004. Lethality to human cancer cells through massive chromosome loss by inhibition of the mitotic checkpoint. *Proc. Natl. Acad. Sci. U. S. A.* **101**: 8699–8704.

Kunimoto K, Nojima H, Yamazaki Y, Yoshikawa T, Okanoue T, Tsukita S. 2009. Involvement of IQGAP3, a regulator of Ras/ERK-related cascade, in hepatocyte proliferation in mouse liver regeneration and development. *J. Cell. Physiol.* **220**: 621–631.

Lee CG, Hague LK, Li H, Donnelly R. 2004. Identification of toposome, a novel multisubunit complex containing topoisomerase IIα. *Cell Cycle* **3**: 638–647.

Lim CB, Zhang D, Lee CG. 2006. FAT10, a gene up-regulated in various cancers, is cell-cycle regulated. *Cell Div.* **1**: 20.

Lincet H, Poulain L, Remy JS, Deslandes E, Duigou F, Gauduchon P, Staedel C. 2000. The p21$^{cip1/waf1}$ cyclin-dependent kinase inhibitor enhances the cytotoxic effect of cisplatin in human ovarian carcinoma cells. *Cancer Lett.* **161**: 17–26.

Livak KJ, Schmittgen TD. 2001. Analysis of relative gene expression data using real-time quantitative PCR and the $2^{-\Delta\Delta C}{}_{T}$ method. *Methods* **25**: 402–408.

Malmlöf M, Roudier E, Högberg J, Stenius U. 2007. MEK-ERK-mediated phosphorylation of Mdm2 at Ser-166 in hepatocytes. Mdm2 is activated in response to inhibited Akt signaling. *J. Biol. Chem.* **282**: 2288–2296.

Mattila R, Alanen K, Syrjänen S. 2007. Immunohistochemical study on topoisomerase IIα, Ki-67 and cytokeratin-19 in oral lichen planus lesions. *Arch. Dermatol. Res.* **298**: 381–388.

Mayo LD, Donner DB. 2002. The PTEN, Mdm2, p53 tumor suppressor-oncoprotein network. *Trends Biochem. Sci.* **27**: 462–467.

Milde-Langosch K, Goemann C, Methner C, Rieck G, Bamberger AM, Löning T. 2001. Expression of Rb2/p130 in breast and endometrial cancer: correlations with hormone receptor status. *Br. J. Cancer* **85**: 546–551.

NTP. 1993a. NTP Toxicology and Carcinogenesis Studies of Acetaminophen (CAS No. 103–90-2) in F344 Rats and B6C3F1 Mice (Feed Studies). *Natl. Toxicol. Program Tech. Rep. Ser.* **394**: 1–274.

NTP. 1993b. NTP Toxicology and Carcinogenesis Studies of Promethazine Hydrochloride (CAS No. 58-33-3) in F344/N Rats and B6C3F1 Mice (Gavage Studies). *Natl. Toxicol. Program Tech. Rep. Ser.* **425**: 1–272.

NTP. 2000. Toxicology and carcinogenesis studies of methyleugenol (CAS NO. 93–15-2) in F344/N rats and B6C3F1 mice (gavage studies). *Natl. Toxicol. Program Tech. Rep. Ser.* **491**: 1–412.

Patil M, Pabla N, Dong Z. 2013. Checkpoint kinase 1 in DNA damage response and cell cycle regulation. *Cell. Mol. Life Sci.* **70**: 4009–4021.

Rees KR, Rowland GF, Ross HF. 1962. The metabolism of isolated rat-liver nuclei during chemical carcinogenesis. 2. 2-Acetylamidofluorene, α-naphthyl isothiocyanate and 20, 40-dimethyl-4-dimethylaminoazobenzene. *Biochem. J.* **82**: 347–352.

Riehle KJ, Campbell JS, McMahan RS, Johnson MM, Beyer RP, Bammler TK, Fausto N. 2008. Regulation of liver regeneration and hepatocarcinogenesis by suppressor of cytokine signaling 3. *J. Exp. Med.* **205**: 91–103.

Rodriguez R, Meuth M. 2006. Chk1 and p21 cooperate to prevent apoptosis during DNA replication fork stress. *Mol. Biol. Cell* **17**: 402–412.

Scholzen T, Gerdes J. 2000. The Ki-67 protein: from the known and the unknown. *J. Cell. Physiol.* **182**: 311–322.

Sherr CJ, Roberts JM. 1995. Inhibitors of mammalian G1 cyclin-dependent kinases. *Genes Dev.* **9**: 1149–1163.

Speidel D. 2015. The role of DNA damage responses in p53 biology. *Arch. Toxicol.* (*in press*) *DOI*: 10.1007/s00204-015-1459-z

Tamano S. 2010. Carcinogenesis risk assessment of chemicals using medium-term carcinogenesis bioassays. *Asian Pacific J. Cancer Prev.* **11**: 4–5.

Taniai E, Hayashi H, Yafune A, Watanabe M, Akane H, Suzuki K, Mitsumori K, Shibutani M. 2012a. Cellular distribution of cell cycle-related molecules in the renal tubules of rats treated with renal carcinogens for 28 days: relationship between cell cycle aberration and carcinogenesis. *Arch. Toxicol.* **86**: 1453–1464.

Taniai E, Yafune A, Hayashi H, Itahashi M, Hara-Kudo Y, Suzuki K, Mitsumori K, Shibutani M. 2012b. Aberrant activation of ubiquitin D at G_2 phase and apoptosis by carcinogens that evoke cell proliferation after 28-day administration in rats. *J. Toxicol. Sci.* **37**: 1093–1111.

Theng SS, Wang W, Mah WC, Chan C, Zhuo J, Gao Y, Qin H, Lim L, Chong SS, Song J, Lee CG. 2014. Disruption of FAT10-MAD2 binding inhibits tumor progression. *Proc. Natl. Acad. Sci. U. S. A.* **111**: E5282–5291.

Uchida C, Miwa S, Kitagawa K, Hattori T, Isobe T, Otani S, Oda T, Sugimura H, Kamijo T, Ookawa K, Yasuda H, Kitagawa M. 2005. Enhanced Mdm2 activity inhibits pRB function via ubiquitin-dependent degradation. *EMBO J.* **24**: 160–169.

Uehara T, Minowa Y, Morikawa Y, Kondo C, Maruyama T, Kato I, Nakatsu N, Igarashi Y, Ono A, Hayashi H, Mitsumori K, Yamada H, Ohno Y, Urushidani T. 2011. Prediction model of potential hepatocarcinogenicity of rat hepatocarcinogens using a large-scale toxicogenomics database. *Toxicol. Appl. Pharmacol.* **255**: 297–306.

Weaver BA, Cleveland DW. 2005. Decoding the links between mitosis, cancer, and chemotherapy: The mitotic checkpoint, adaptation, and cell death. *Cancer Cell* **8**: 7–12.

Woessner RD, Mattern MR, Mirabelli CK, Johnson RK, Drake FH. 1991. Proliferation- and cell cycle-dependent differences in expression of the 170 kilodalton and 180 kilodalton forms of topoisomerase II in NIH-3 T3 cells. *Cell Growth Differ.* **2**: 209–214.

Yafune A, Taniai E, Morita R, Nakane F, Suzuki K, Mitsumori K, Shibutani M. 2013a. Expression patterns of cell cycle proteins in the livers of rats treated with hepatocarcinogens for 28 days. *Arch. Toxicol.* **87**: 1141–1153.

Yafune A, Taniai E, Morita R, Hayashi H, Suzuki K, Mitsumori K, Shibutani M. 2013b. Aberrant activation of M phase proteins by cell proliferation-evoking carcinogens after 28-day administration in rats. *Toxicol. Lett.* **219**: 203–210.

Yamamoto Y, Matsuyama H, Kawauchi S, Matsumoto H, Nagao K, Ohmi C, Sakano S, Furuya T, Oga A, Naito K, Sasaki K. 2006. Overexpression of polo-like kinase 1 (PLK1) and chromosomal instability in bladder cancer. *Oncology* **70**: 231–237.

Yuan B, Xu Y, Woo JH, Wang Y, Bae YK, Yoon DS, Wersto RP, Tully E, Wilsbach K, Gabrielson E. 2006. Increased expression of mitotic checkpoint genes in breast cancer cells with chromosomal instability. *Clin. Cancer Res.* **12**: 405–410.

Zhang H, Chen X, Jin Y, Liu B, Zhou L. 2012. Overexpression of Aurora-A promotes laryngeal cancer progression by enhancing invasive ability and chromosomal instability. *Eur. Arch. Otorhinolaryngol.* **269**: 607–614.

Toxicology 331 (2015) 125–135

Contents lists available at ScienceDirect

Toxicology

journal homepage: www.elsevier.com/locate/toxicol

Chemical structure-related mechanisms underlying *in vivo* genotoxicity induced by nitrofurantoin and its constituent moieties in *gpt* delta rats

Aki Kijima [a], Yuji Ishii [a], Shinji Takasu [a], Kohei Matsushita [a], Ken Kuroda [a], Daisuke Hibi [a], Yuta Suzuki [a], Takehiko Nohmi [b], Takashi Umemura [a,*]

[a] Division of Pathology, National Institute of Health Sciences, Tokyo 158-8501, Japan
[b] Biological Safety Research Center, National Institute of Health Sciences, Tokyo 158-8501, Japan

ARTICLE INFO

Article history:
Received 17 February 2015
Received in revised form 3 March 2015
Accepted 7 March 2015
Available online 12 March 2015

Keywords:
Nitrofurantoin
gpt delta rat
In vivo mutagenicity
Kidney

ABSTRACT

Nitrofurans are antimicrobial compounds containing a nitro group at the 5-position of the furan ring and an amine or hydrazide side chain derivative. One member of the nitrofurans, nitrofurantoin (NFT), is a renal carcinogen in male rats despite its still controversial genotoxicity. We investigated chemical structure-related modes of action of NFT, and reporter gene mutation assays for NFT and its constituent moieties were performed. NFT, 5-nitro-2-furaldehyde (NFA), or 1-aminohydantoin (AHD) was administered to male F344 *gpt* delta rats by gavage for 4 or 13 weeks at a carcinogenic or the maximum tolerated dose. NFT caused a significant increase in *gpt* mutant frequency (MF) at 13 weeks with G-base substitution mutations. An increase in *gpt* MF was also observed in the NFA-treated group at 13 weeks, but not in the AHD-treated group. 8-Hydroxydeoxyguanosine (8-OHdG) levels in the kidney DNA of NFT-treated rats were significantly increased after 4 weeks. NFT caused accumulation of hyaline droplets indicated by positive immunostaining and western blot analysis for α_{2u}-globulin in the proximal tubules. An additional study, in which female *gpt* delta rats were given NFT at the same dose used for males, was performed to mitigate the effect of α_{2u}-globulin. NFT exerted the same effects on female rat kidneys to the same extent as males in terms of *gpt* MF and 8-OHdG level. Thus, it is highly probable that the structure of the nitro furan plays a key role in NFT-induced genotoxicity and genotoxic mechanisms including oxidative DNA damage are involved in NFT-induced renal carcinogenesis. α_{2u}-globulin-mediated nephropathy may be a prerequisite for NFT-induced renal carcinogenesis in male rats, and additionally NFT could be a latent carcinogen in female rats and other animal species.

1. Introduction

Nitrofurans are compounds containing a nitro group at the 5-position of the furan ring and an amine or hydrazide side chain derivative that are used as human and animal antimicrobial and food additives. Since a number of studies have demonstrated that some nitrofurans have genotoxic and/or carcinogenic potential in particular, the use of nitrofurans including furaltadone, furazolidone, nitrofurazone, and nitrofurantoin (IARC, 1974, 1983, 1990a,b) as food additives or veterinary medicines is prohibited in Japan. The mechanisms underlying the genotoxicity or carcinogenicity of these compounds are still unclear. Nevertheless, new nitrofuran agents with various hydrazide derivatives on the side chain are still being developed (Zorzi et al., 2014; Fleck et al., 2014). Thus, clarifying the underlying mechanisms of this class of chemicals is an urgent matter for assessment of human risk.

The antibacterial activities of nitrofurans are known to involve formation of reactive oxygen species (ROS) and/or reactive intermediates resulting from reduction of the nitro group (Bartel et al., 2009; Boelsterli et al., 2006; Chung et al., 2011), in common with other nitro compounds such as nitro heterocyclic antimicrobials, consequently inducing oxidative modifications of DNA/protein in target bacteria. Likewise, it is thought that these detrimental functions of nitrofurans also affect mammal hosts causing cytotoxicity, genotoxicity, and carcinogenicity (Hiraku et al., 2004; Jin et al., 2011; McCalla, 1983). However, despite nitrofurans possessing similar basic structures, there is variability in the degree of their toxicity together with a variation in target

* Corresponding author. Tel.: +81 3 3700 9819; fax: +81 3 3700 1425.
E-mail address: umemura@nihs.go.jp (T. Umemura).

http://dx.doi.org/10.1016/j.tox.2015.03.003
0300-483X/

organ sites, which indicates that not only the common structure, nitrofuran, but also amine or hydrazide derivatives on the side chain may be responsible for their toxicity. In addition, there might be effects of the side chain structure on the properties of the nitrofurans.

Nitrofurantoin (*N*-(5-nitro-2-furfurylidene)-1-aminohydantoin; NFT) is generated by the condensation of 5-nitro-2-furaldehyde (NFA) and 1-aminohydantoin (AHD) (Fig. 1), and it is used extensively as a prophylactic for urinary tract infections in humans and animals (IARC, 1990b; Wagenlehner et al., 2011; Maaland and Guardabassi, 2011). The National Toxicology Program (1989) has reported on the carcinogenicity of NFT in the kidneys of male F344 rats. However, there are inconsistent results between *in vitro* and *in vivo* genotoxicity tests. Although the rat micronucleus test showed negative results, in the test for detecting DNA strand breaks, many positive results were shown using rat liver, kidney, lung, spleen, and mice bone marrow cells (IARC, 1990b). An *in vivo* mutation assay using the kidneys of Big Blue mice gave a positive result with significant incremental incidence of the G:C-T:A transversion mutation (Quillardet et al., 2006) despite mouse kidney not being the carcinogenic target site of NFT. Thus, although possible participation of genotoxic mechanisms in NFT-induced renal carcinogenesis has been suspected, there is insufficient evidence to clarify the mode of action.

In the present study, to evaluate the chemical structure-related carcinogenic mechanism of NFT, we performed a reporter gene mutation assay with the kidneys of male *gpt* delta rats (Matsushita et al., 2015; Nohmi et al., 2000) administered NFT (parent compound), NFA (a constituent compound of NFT with the nitrofuran group) or AHD (a metabolite of NFT with a hydrazide group). Additionally, the level of 8-hydroxydeoxyguanosine (8-OHdG), one type of oxidized DNA damage (Williams and Jeffrey, 2000), in the kidney DNA was quantitatively measured. An additional study using female *gpt* delta rats was performed to clarify the relationship between oxidative DNA damage and *in vivo* genotoxicity induced by NFT.

2. Materials and methods

2.1. Chemicals and reagents

NFT ($C_8H_6N_4O_5$, MW 238.2, CAS No. 67-20-9), NFA ($C_5H_3NO_4$, MW 141.08, CAS No. 698-63-5) and AHD ($C_3H_5N_3O_2$·HCl, MW 151.55, CAS No. 2827-56-7) were purchased from Sigma–Aldrich Co., Llc. (St. Louis, MO, USA), and were suspended in 0.5 w/v% methyl cellulose 400 cP solution (Wako Pure Chemical Industries, Ltd., Osaka, Japan). Suspensions of the test chemicals were used at a volume of 10 ml/kg body weight (BW), based on body weight on the day of administration to *gpt* delta rats.

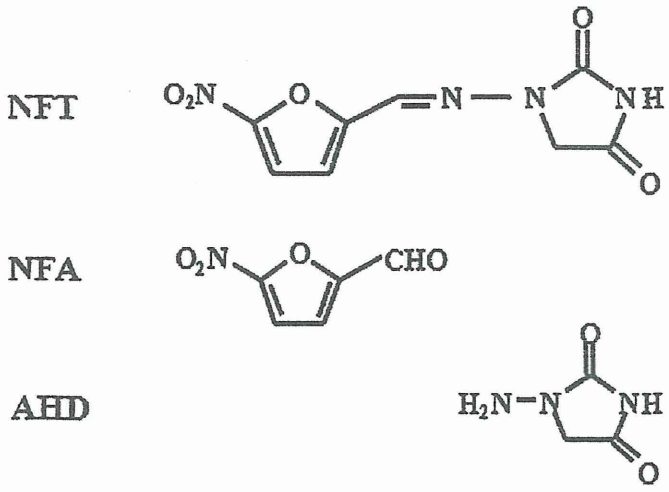

Fig. 1. Chemical structure of NFT, NFA and AHD.

2.2. Animals and housing conditions

Five-week-old F344 *gpt* delta rats were obtained from Japan SLC, Inc. (Shizuoka, Japan). After the animals had been acclimated for one week, housed 2–3 rats in a cage with hardwood chips, and food (CRF-1, solid form; Oriental yeast Co., Ltd., Tokyo, Japan) and distilled water provided *ad libitum*, they were kept under controlled conditions (temperature 23 ± 2 °C, humidity 55 ± 5%, air changed 12 times per hour, and lighting 12 h light/dark cycle). This study was approved by the Animal Care and Utilization Committee of the National Institute of Health Sciences (Tokyo, Japan).

2.3. Experimental design

In experiment 1, male *gpt* delta rats were randomized into four groups (vehicle control, NFT-treated, NFA-treated, and AHD-treated groups) of 10 rats, with five rats from each group sacrificed at week 4 and week 13. In experiment 2, female *gpt* delta rats were allocated to two groups (vehicle control and NFT-treated groups) of 5 rats that were sacrificed at week 13. NFT, NFA, and AHD were administered by gavage for five consecutive days, and the control group was administered vehicle alone. For daily doses, NFT at 125 mg/kg BW, which corresponded to the value in renal carcinogenic levels of the dietary administration study (NTP, 1989) were calculated using a conversion value of Joint FAO/WHO Expert Committee on Food Additives (JECFA; IPCS, EHC70). A dose-determination study with NFA and AHD was performed using the same molar concentrations as the NFT dose. NFA and AHD were set to 50 and 80 mg/kg BW as the maximum-tolerated doses, respectively. In experiment 2, NFT was administered to female rats at the same dose as was used for males. At autopsy, all test animals were euthanized with isofluran (Mylan Inc., Tokyo, Japan), and blood samples were collected. Kidneys were collected and their weights were measured. A portion of the kidney tissues were frozen with liquid nitrogen and were stored at −80 °C, for use in the analysis by the *in vivo* mutation assay, western blotting, and 8-OHdG measurement. The remaining kidney tissues were fixed in 10% formalin-buffer and were used in a histopathology and immunostaining examination.

2.4. In vivo mutation assays

6-Thioguanine (6-TG) and Spi⁻ selection were performed as described previously (Nohmi et al., 2000). In brief, genomic DNA was extracted from kidney tissues of the male or female rats, and lambda EG10 DNA (48 kb) was rescued as the lambda phage through *in vitro* packaging. For 6-TG selection, the packaged phages were incubated with *Escherichia coli* YG6020 that expressed Cre recombinase and were converted to plasmids carrying *gpt* and chloramphenicol acetyltransferase. Infected cells were mixed with molten soft agar and were poured onto agar plates containing chloramphenicol and 6-TG. For determination of the total number of rescued plasmids, 3000-fold diluted phages were infected with YG6020, and the suspension was poured into plates containing chloramphenicol without 6-TG. These plates were incubated at 37 °C, and positive colonies were counted on day 3, and recovered on day 4. The *gpt* mutant frequency (MF) was calculated by dividing the number of *gpt* mutants by the total

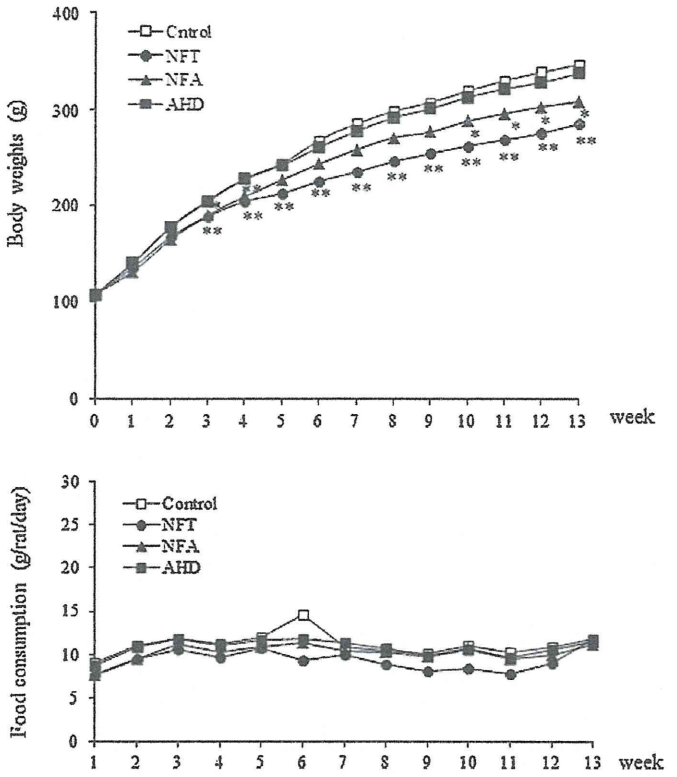

Fig. 2. Growth curves and food consumption for male *gpt* delta rats treated with NFT, NFA or AHD for 13 weeks. *,** Significantly different ($P < 0.05$, 0.01) from the control group by Dunnett's test.

number of rescued phages. In collected positive colonies, the *gpt* mutant spectra were characterized. To characterize the spectrum of the *gpt* mutants, a 739 bp DNA fragment containing the 456 bp coding region of the *gpt* gene was amplified by PCR using the collected positive colonies as a template DNA, as previously described (Matsushita et al., 2015). The amplified DNA was separated by agarose gel electrophoresis, which confirmed the amplification size, and DNA sequences were analyzed at the Dragon Genomics Center of Takara Bio (Mie Japan). For Spi^- selection, packaging phages were incubated with *E.coli* XL-1 Blue MRA (for survival titration) and *E. coli* XL-1 Blue MRA P2 (for mutant selection). Infected cells were mixed with molten soft agar and were poured onto lambda-trypticase agar plates. The plates were incubated at 37 °C for one day. Plaques that appeared were collected and suspended in SM buffer. To confirm the Spi^- phenotype of false-positives, the suspensions were spotted on 3 types of plates (XL-Blue, XL-Blue-P2, and WL95-P2 strains). Samples with clear plaque in all of the plate types were confirmed to be the true Spi^- mutation.

Table 1
Final body and kidney weights of male *gpt* delta rats treated with NFT, NFA, or AHD for 4 or 13 weeks.

	Final body weights (g)	Kidney weights	
		Absolute (g)	Relative (g%)[a]
4 Weeks			
Control	223.4 ± 6.8 [b]	1.49 ± 0.08	0.67 ± 0.04
NFT	202.3 ± 13.4	1.50 ± 0.06	0.74 ± 0.02*
NFA	206.6 ± 19.0	1.43 ± 0.17	0.69 ± 0.02
AHD	227.9 ± 9.1	1.53 ± 0.07	0.67 ± 0.01
13 Weeks			
Control	347.3 ± 21.9	1.87 ± 0.12	0.54 ± 0.01
NFT	285.8 ± 7.7**	1.92 ± 0.09	0.67 ± 0.02*
NFA	308.9 ± 12.2*	1.91 ± 0.07	0.62 ± 0.01*
AHD	338.0 ± 25.9	1.86 ± 0.10	0.55 ± 0.03

*,**Significantly different ($P < 0.05$, 0.01) from the control group by Dunnett's or Steel's test.
[a] Kidney weight-to-body weight ratios (relative weights) are given as g organ weight/g body weight.
[b] Means ± SD.

Table 2
gpt MFs in the kidneys of male *gpt* delta rats treated with NFT, NFA, or AHD for 4 weeks.

Treatment	Animal No.	Cm^R colonies ($\times 10^5$)	6-TG^R and Cm^R colonies	MF ($\times 10^{-5}$)	Mean ± SD
Control	1	10.7	3	0.28	
	2	17.8	3	0.17	
	3	27.5	2	0.07	
	4	15.7	3	0.19	
	5	16.7	2	0.12	0.17 ± 0.08
NFT	11	13.4	9	0.67	
	12	11.5	3	0.26	
	14	23.9	13	0.54	
	15	14.8	9	0.61	0.52 ± 0.18
NFA	21	16.3	3	0.18	
	22	14.2	4	0.28	
	24	15.6	2	0.13	
	25	10.8	9	0.83	0.36 ± 0.32
AHD	31	8.0	2	0.25	
	32	12.2	3	0.25	
	33	29.2	6	0.21	
	34	22.1	6	0.27	
	35	11.9	13	1.09	0.41 ± 0.38

Cm^R, chloramphenicol resistant; 6-TG^R, 6-thioguanine resistant; and MF, mutant frequency.

Table 3
gpt MFs in the kidneys of male *gpt* delta rats treated with NFT, NFA, or AHD for 13 weeks.

Treatment	Animal No.	Cm^R colonies ($\times 10^5$)	6-TG^R and Cm^R colonies	MF ($\times 10^{-5}$)	Mean ± SD
Control	6	4.5	1	0.22	
	7	5.3	1	0.19	
	8	4.1	3	0.73	
	9	25.1	9	0.36	
	10	6.6	3	0.45	0.39 ± 0.22
NFT	17	1.3	5	3.83	
	18	2.4	2	0.84	
	19	4.2	8	1.89	
	20	7.7	10	1.31	1.97 ± 1.32**
NFA	26	4.1	5	1.23	
	27	3.6	2	0.56	
	28	14.6	19	1.30	
	29	3.2	3	0.95	
	30	3.4	3	0.88	0.99 ± 0.30*
AHD	36	3.5	2	0.57	
	37	4.0	1	0.25	
	38	8.2	1	0.12	
	39	4.5	2	0.44	
	40	3.8	3	0.78	0.43 ± 0.26

Cm^R, chloramphenicol resistant; 6-TG^R, 6-thioguanine resistant; and MF, mutant frequency.
*,** Significantly different ($P < 0.05$, 0.01) from the control group by Dunnett's test.